2. Peebles, F. N., and H. J. Garber, *Chem. Eng. Progr.*, **49**, 2 (Feb., 1953).
3. Davies, R. M., and G. Taylor, *Proc. Royal Soc. (London)*, **200A**, 375-390 (1950).
4. Levich, V. G., "Physicochemical Hydrodynamics," Prentice-Hall, Englewood Cliffs, N. J. (1962).
5. Harmathy, T. Z., *A.I.Ch.E. J.*, **6**, No. 2, 281 (1960).
6. Lamb, H., "Hydrodynamics," 6 ed., Dover, New York (1932).
7. Jontz, P. D., and J. E. Myers, *A.I.Ch.E. J.*, **6**, No. 34 (1960).

Manuscript received August 18, 1966; revision received November 29, 1966; paper accepted December 1, 1966.

Flow of Viscoelastic Fluids Past a Flat Plate

R. A. HERMES and A. G. FREDRICKSON

University of Minnesota, Minneapolis, Minnesota

The flow of viscoelastic fluids past a flat plate has been investigated. Experimental studies were performed with aqueous solutions of sodium carboxymethylcellulose used as viscoelastic fluids and corn syrup as a viscous Newtonian fluid. It was observed that the flow patterns of elastic and inelastic fluids are markedly different. Tracer particles placed in the approaching viscoelastic fluids to follow their motion were seen to first decelerate and then to accelerate until a nearly constant velocity was reached. On the other hand tracer particles in the Newtonian fluid were observed merely to decelerate smoothly to the constant velocity.

The drag force measured for the viscoelastic fluids was found to be roughly twice that predicted by inelastic models of fluid behavior. Predicted and measured values of the drag force for the Newtonian fluid agreed well.

A discussion of mathematical solutions to the problem of flow of viscoelastic fluids past a flat plate is given. Solutions are obtained for a prototype of flow past a flat plate, the suddenly accelerated flat plate (Stokes' problem) with linear viscoelastic models used. The results from Stokes' problem qualitatively explain the anomalous kinematical behavior and the large drag force.

Many important commercial processes involve the flow of viscoelastic fluids in complex geometries. Although very general constitutive equations have been provided for these fluids (*6, 7, 10*), few engineering problems using them have been solved. The problem considered in this paper is flow of viscoelastic fluids past a flat plate, a prototype of many flow situations encountered in industry. Studies of complex flow situations are important from a fundamental viewpoint also. For viscometric flows the general theory of Coleman and Noll (*6*) can be shown to reduce to the determination of three material functions: a viscosity function and two normal stress differences (*7*). The simple degeneracy of these flows comes about because the kinematical history of a material particle is the same for all past times within its memory. Methods are described in the literature for the measurement of all three of these material functions (*9, 12, 17, 21*). The next step in elucidating the nature of viscoelastic fluids seems to be the study of complex flows where at least some of the degeneracy of laminar shear flows is removed.

Recent results on steady complex flows of non-Newtonian fluids that display viscoelastic properties show conflicting results. In some situations it has been found that solutions of the equations of motion using inelastic, non-Newtonian models are sufficient to describe macroscopic variables of primary engineering interest. For example, Sutterby (*29*) found that laminar converging flow in a conical section could be described by a non-Newtonian, inelastic model he proposed. Likewise Sadowski (*23*) has shown that his data on flow in a packed bed could be described by using the Ellis model. On the other hand, Walters and Savins (*26*) have shown that the flow patterns around a rotating sphere are qualitatively different for a viscoelastic fluid than for an inelastic fluid. Sakiadis (*24, 25*) has done experimental studies on entrance effects into a capillary and found larger pressure losses and a longer entrance length than predicted by inelastic theory. Many other examples could be cited, of course. However, no definite method of predicting the importance of elastic effects a priori has been given. However, one can probably say that the longest relaxation time of the fluid must be of the same order or greater than some characteristic time of the system, if elastic effects are to be of importance. More experimental and theoretical work is needed to establish the conditions under which viscoelastic effects are important.

Recently, attention has been turned to flow past submerged objects (*19, 31*). These flows are important from a fundamental standpoint because they are unsteady in the Lagrangian sense. That is, the kinematic state viewed by a material particle changes as it traverses the object. It is in these flows in which the kinematic history of a material particle changes with time that elastic effects are usually manifested.

THEORY

The problem of flow of purely viscous fluids past a flat plate (boundary-layer flow) has been studied in detail. For Newtonian fluids many solutions, both exact and approximate, are available (*27*). Acrivos et al. (*1, 2*) and Schowalter (*28*) have analyzed this problem for fluids which obey the power law model

R. A. Hermes is with Mobil Oil Corporation, Dallas, Texas.

$$\mathbf{p} = m\left(\frac{1}{2}\Gamma_1:\Gamma_1\right)^{\frac{n-1}{2}}\Gamma_1 \qquad (1)$$

where Γ_1 is twice the symmetric part of the velocity gradient. Schowalter investigated the conditions under which similarity solutions exist and Acrivos et al. computed solutions for various values of the fluid index. Approximate solutions of the Pohlhausen type are also available (*2, 3*). Hermes (*11*) showed that a Pohlhausen approximate solution can be found for a modified version of the Ellis model (*20*):

$$\mathbf{p} = \frac{m_e\eta_0}{m_e + \eta_0\left(\frac{1}{2}\Gamma_1:\Gamma_1\right)^{(1-n_e)/2}}\Gamma_1 \qquad (2)$$

For viscoelastic fluids the only work reported has been concerned with attempts to extend the classical boundary-layer technique to modifications of the second-order fluid (*22, 31*):

$$\mathbf{p} = \eta\,\Gamma_1 + \omega_2\Gamma_1\cdot\Gamma_1 + \omega_3\Gamma_2 \qquad (3)$$

where Γ_2 is the convected time derivative of Γ_1; it is often called the second Rivlin-Ericksen acceleration tensor. White and Metzner (*31*) have simplified the equations of motion for flow past a flat plate by assuming that the equation for the direction perpendicular to the plate can be neglected, that the variation of the normal stress p_{xx} along the direction parallel to the plate is negligible, and that a Prandtl order of magnitude analysis is valid. They then show that similarity solutions to the simplified equations of motion do not exist for the second-order fluid.

Metzner and White (*18*) have applied the second-order fluid boundary-layer analysis to the entrance flow problem. The method used involves an approximate solution with the assumption that the velocity profiles are nearly similar. Their results show increases or decreases in the entrance length dependent on values chosen for the elasticity parameters.

While these attempts which use the second-order type of model serve as a starting point, they are subject to such severe criticism that few conclusions can be drawn from them. First of all, the results depend on the validity of the assumed kinematical behavior. In all these schemes it is assumed that the kinematical behavior and the relative orders of magnitude of various quantities are similar to those found for Newtonian fluids. The assumption of similarity of velocity profiles in any approximate scheme has doubtful basis. For Newtonian fluids similarity of the velocity profiles follows from the fact that the system has no characteristic length. For viscoelastic fluids however the fluid has a nonzero characteristic time. The presence of this characteristic time would be expected to be manifested as an equivalent characteristic length. In this case similarity of velocity profiles should not be anticipated.

The validity of the second-order model in this situation is also doubtful. The second-order model results from assuming that the kinematics of all past times within the fluid's memory can be described by a truncated Taylor series about the present time. Since flow past a flat plate causes a material particle to experience rapidly changing kinematical states (at least in neighborhood of the leading edge), a Taylor series of a few terms probably fails to give an accurate approximation of past kinematical happenings. This conclusion has been reached in other instances where the second-order model has been used in situations where the kinematical happenings as viewed by a material particle change rapidly (*5, 8*).

Since the use of the second-order model discussed above seems to be of limited value in predicting the behavior near the leading edge, a method using integral (long memory) constitutive equations is needed. Because of the complexity of the kinematical relationships in this flow, the direct use of integral constitutive equations is out of the question also. Another approach is to examine the unsteady state analog of this problem, the suddenly accelerated flat plate (Stokes' first problem). This technique simplifies the mathematical problem considerably, since implicit nonlinear time dependence is replaced by linear explicit time dependence. The solution of this problem for Newtonian fluids gives impetus to the solution for classical boundary-layer flow (*27*). Thus, a comparison of the solutions to Stokes' problem with linear integral viscoelastic fluid models used with those from the corresponding Newtonian model may be useful in giving a qualitative idea of the effects of elasticity in flows of viscoelastic fluids past a flat plate. In particular, the wall shear stress as a function of time for Stokes' problem is analogous to the wall shear stress as a function of distance down the plate for the flow past a flat plate problem.

Consider a flat wall of infinite extent above which is an infinite sea of fluid at rest. Let the x coordinate lie along the plate; the y coordinate, normal to the plate; and the origin, in the wall. At time zero the wall is suddenly set into motion in the x direction with constant velocity. Suppose the fluid is described by the linear model

$$p^{ij} = \int_{-\infty}^{t}\psi(t-t')\frac{\partial x^i}{\partial X^m}\frac{\partial x^j}{\partial X^n}\Gamma_1^{mn}(X^p,t')\,dt' \qquad (4)$$

where ψ is the relaxation function (*9*). The x's denote current coordinates, while the X's represent material coordinates. The equations of motion reduce to

$$\rho\frac{\partial u}{\partial t} = \frac{\partial p_{xy}}{\partial y} \qquad (5)$$

with boundary conditions

$$u(y,0) = 0 \qquad (6a)$$

$$u(0,t) = u,\ t > 0 \qquad (6b)$$

$$\lim_{y\to\infty} u(y,t) = 0 \qquad (6c)$$

By a straightforward method where Laplace transforms are used, this system of equations can be solved for the shear stress at the wall:

$$\bar{p}_{xy}(0,s) = -U\sqrt{\frac{\rho\bar{\psi}(s)}{s}} \qquad (7)$$

For illustrative purposes a good choice for the relaxation function is the three-constant model

$$\psi(t) = G_N\delta(t) + G_Me^{-t/\lambda} \qquad (8)$$

Fredrickson and co-workers (*13, 14, 30*) have found that this model correlates experimental data reasonably well. Other choices lead to the same qualitative results (*11*). Using this model for the relaxation function, we may invert the Laplace transform of the wall shear stress to get

$$p_{xy}(0,t) = -U\sqrt{G_N\rho}\left\{a\int_0^t \exp\left[-a(t-t')\right]\right.$$

$$\left.\left[I_1\{a(t-t')\} + I_0\{a(t-t')\}\right]\frac{e^{-t'/\lambda}}{\pi t'}\,dt' + \frac{e^{-t/\lambda}}{\pi t}\right\} \qquad (9)$$

with

$$a = G_M/2\lambda G_N \qquad (10)$$

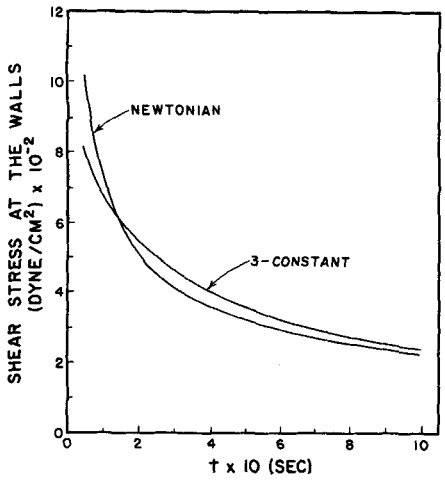

Fig. 1. Wall shear stress vs. time for three-constant model and Newtonian model.

The convergence of the convolution integral and associated numerical methods are discussed in detail by Hermes (*11*). Calculations with typical values for the constants used are shown in Figure 1. These values were (c.g.s. units): $\eta = 16$, $\lambda = 0.20$, $G_N = 4$, $G_M = 60$, and $U = 100$. The Newtonian results are calculated with the requirement that

$$\eta = \int_0^\infty \psi(t)dt \qquad (11)$$

It is seen from Figure 1 that at times less than the order of the relaxation time of the fluid, the viscoelastic model predicts lower stresses than for the corresponding Newtonian fluid. However, at times of the order of and somewhat greater than the relaxation time of the fluid, the viscoelastic model predicts larger stresses than the Newtonian fluid. Finally, at large times the models predict nearly identical stresses. Transforming these results to boundary-layer flow would seem to indicate that most of the elastic effects occur near the leading edge of the plate; at distances farther down the place, inelastic models are sufficient. This is not surprising, since it is at the leading edge that high shear rates are suddenly applied to the fluid. The shear rate is then expected to decrease as the fluid progresses down the plate. Near the leading edge, the corresponding shear stress for viscoelastic fluids is less than that of the inelastic fluid because the shear-free flow upstream from the plate is still within the memory of the viscoelastic fluid. As the fluid progresses down the plate the stress (relative to that of the inelastic fluid) increases as shear rates larger than the current rate are within the fluid's memory. At larger distances down the plate the shear rate changes very slowly, and thus the resulting stresses are about the same for the elastic and corresponding inelastic fluid.

It is impossible to draw any quantitative conclusions from these results, since the model assumed is linear and an actual fluid would show nonlinear behavior at shear rates of interest. Likewise, the problem solved is only a prototype problem. Nevertheless, the results are a starting point in considering the effects of fluid elasticity and may be of interest in pointing to the type of effects one can expect to encounter.

EXPERIMENTAL PROCEDURE

The performance of the classical boundary-layer experiment requires that the plate be mounted in a large trough so that the constant approach velocity assumption and infinite boundary conditions of the mathematical problem can be approximated. For this to be accomplished larger pumping capacities than those that were available to us are required. Since the experimental results sought in this study were conceptual in nature, a freely falling jet effluxing from a 1½-in. pipe and impinging on a flat plate was used to simulate the usual boundary-layer experiment. In this manner the mathematical assumptions would be approximated near the leading edge of the plate.

The pumping system consisted of a Moyno 6M4 pump driven by a 5-hp., variable-speed motor. Velocity profiles in the free jet were measured by the tracer particle method described below to determine the distance from the pipe exit required for the profile to be relaxed. This distance was found to be a maximum of about 3 cm. But, to be certain, the plate was mounted approximately 6 cm. downstream from the pipe exit.

Fluids Used

Solutions of 0.7, 1.0, and 1.3% CMC (Hercules Powder Company) were used as viscoelastic fluids. Diluted solutions of Globe Brand corn syrup (Corn Products), a Newtonian fluid, were used to ensure that any observed anomalies were due to the viscoelastic nature of the fluids, rather than artifacts of the method used. Table 1 lists the fluids used and their properties.

Kinematical Measurements

The kinematics of the flow were determined by taking motion pictures of tracer particles injected at various positions upstream from the plate. The apparatus is shown in Figure 2. The motion pictures were then read frame-by-frame to get the displacement-time relationships for various streamlines. A Bolex H16 Reflex 16-mm. camera was used at speeds up to about 90 frames/sec. with individual frames exposed for about 1/500 sec. The tracer particles introduced were small clusters of hydrogen bubbles produced by inserting a thin wire into the stream, making it cathodic to a d.c. supply, and pulsing the current. This method was first introduced by Clutter et al. (*4*) and was studied in detail by Kline et al. (*15*). The method used here was similar to that of Kline and co-workers. Only the tip of a thin insulated copper wire (diameter 0.006 in.) was bared. This produced a thin but dense cluster of bubbles. An electronic pulsing device capable of producing pulses with duration from 10 to 700 msec. at frequencies from 0.2 to 3 sec.$^{-1}$ was used. The thin wire was mounted on a rack and pinion and inserted diametrically into the jet to the position desired. The electrical system was grounded through the piping system. The plate used (0.584 cm. long and 0.023 cm. thick) was made from 1/64-in. stainless steel stock, polished, and sharpened to a knife edge. The plate was inserted approximately ⅞ of the way through the jet so that the interface through which the viewing took place was not disturbed. Corrections for refraction could then be made easily. The length required so that the boundary-layer thickness at the exit end of the plate was less than the jet radius

TABLE 1. FLUIDS USED

Fluid No.	Composition	Power law parameters c.g.s. units m	n	Ellis model parameters c.g.s. units m_e	n_e	η_0
1	0.7% CMC in water	8.9	0.57	—	—	—
2	1.0% CMC in water	13.4	0.58	—	—	—
3	1.3% CMC in water	54.7	0.57	—	—	—
4	90% corn syrup, 10% water	—	—	—	—	6.33
5	83% corn syrup, 17% water	—	—	—	—	2.20
6	0.7% CMC in water	6.1	0.58	29.1	0.40	1.37
7	1.0% CMC in water	24.8	0.49	42.1	0.43	6.5
8	1.3% CMC in water	54.7	0.45	57.2	0.45	17.2

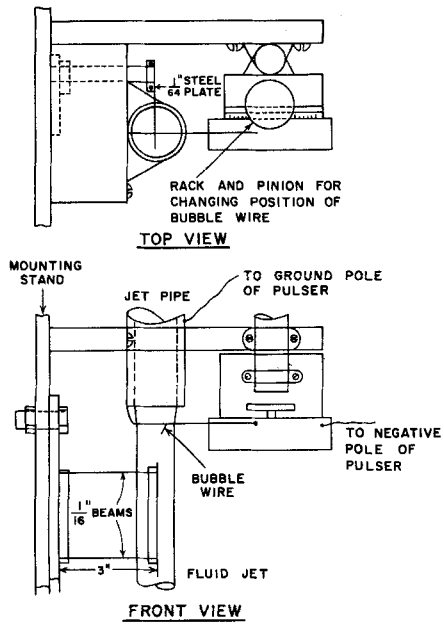

Fig. 2. Experimental apparatus for kinematical measurements.

was calculated by using the viscous fluid parameters. Approximately one-half of this calculated length was used.

Measurements were made along four streamlines at varying distances from the plate. Several particles were followed along each streamline. Complete details of the technique are available elsewhere (*11*).

Drag Force Measurement

The total drag on the plate was measured by mounting the plate on flexure beams and converting the resulting displacement to voltage with a linear variable differential transformer (020-ML from Schaevitz Engineering Company). Figure 3 shows the apparatus. After each run the system was calibrated by hanging various weights on the plate. Beams of various thicknesses could be used to control the sensitivity of the instrument.

Edge and end effects were corrected by inserting the plate into the jet at two (or more) positions and subtracting (or extrapolating). This procedure requires that the edge and/or end region not extend over the entire width of the plate for any positions used (see below).

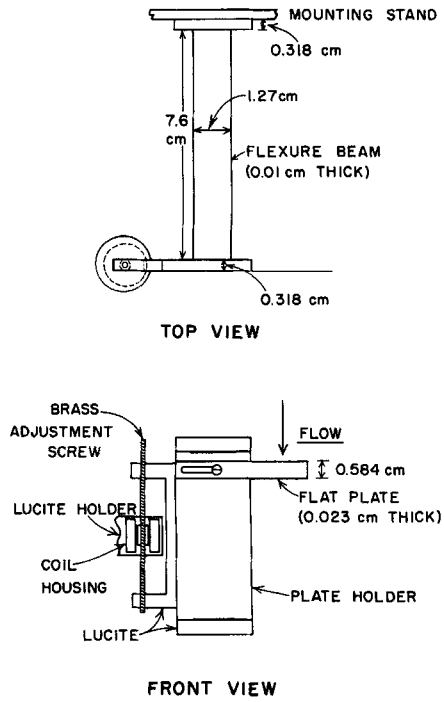

Fig. 3. Experimental apparatus for drag force measurement.

Measurement of Viscous Fluid Parameters

The viscous fluid properties of the fluids used in the drag force experiments were determined from data taken on a cone and plate viscometer. In addition the limiting viscosity was measured with a falling sphere viscometer by using the method of McEachern (*16*). These measurements were made at the University of Wisconsin by Dr. John D. Huppler. The viscometric data were fit to various models by least-squares techniques. For the fluids used in the kinematical measurements, data were taken on a small capillary tube viscometer, and no calculations were made from these data. These fluids are designated 1-3 in Table 1.

RESULTS

Kinematical Measurements

The kinematical measurements were designed to obtain a qualitative and semiquantitative description of the velocity as a function of position for flow of viscoelastic fluids past a flat plate. As mentioned above, the method used was cinematography of tracer particles. The main purpose was to see whether or not unusual effects (that is, effects different from those observed for inelastic fluids) are present.

The data for the particle position vs. time curves were obtained from the movie film by using a pair of dividers in conjunction with a photographed reference scale. Data were read for several frames before the particle reached the plate and all along the plate. Several particles were followed along each streamline so that the nature of the curve could be determined everywhere. The distance scale could be read to an accuracy of about 0.03 cm. The time scale, the time lapse between frames, was determined by reading the stopwatch over a 50-frame interval and finding the average.

Edge effects are produced where the plate enters the jet and end effects are present near the end of the plate in the jet. Likewise, the potential velocity was not constant, but was being accelerated by gravity. Since these effects are of an undetermined importance, measurements were made first for the corn syrup solution (Newtonian fluid). This was done to make sure that anomalous effects were due to the fluid and not the system. Qualitatively, the same results would be expected for the power law (inelastic) fluids and Newtonian fluids. Thus, departure from the qualitative behavior observed for the corn syrup solution can then be interpreted as arising from the elasticity of the fluids.

The particle path vs. time and corresponding streamline curves for four streamlines of the corn syrup run are shown in Figure 4. In these figures U_0 is the velocity at the leading edge of the plate found by measuring the diameter of the jet there and using the pump calibration The distance down the plate from the leading edge is x. The zero of time is chosen arbitrarily for plotting convenience; the slope of the curve is what is important. The slope of these curves at a point is the x component of the velocity. In principle, then, each curve determines the velocity along a streamline. In practice, however, the camera speed was not sufficiently fast to give an accurate determination of the velocity in regions where it changes rapidly. Nevertheless, the qualitative nature can be easily interpreted. A short distance down the plate the velocity

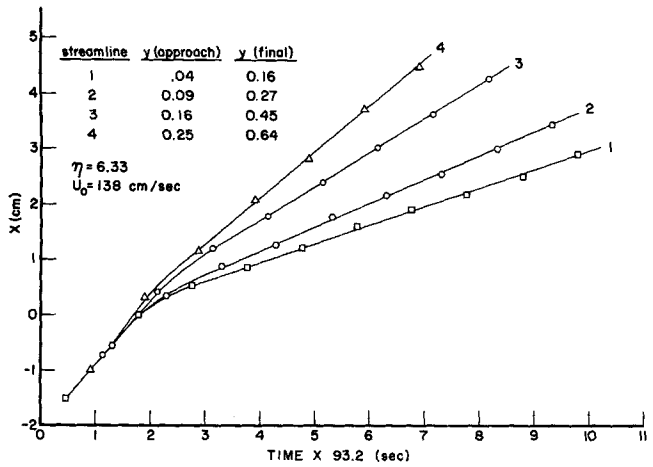

Fig. 4. Particle position vs. time for Newtonian fluid (fluid 4).

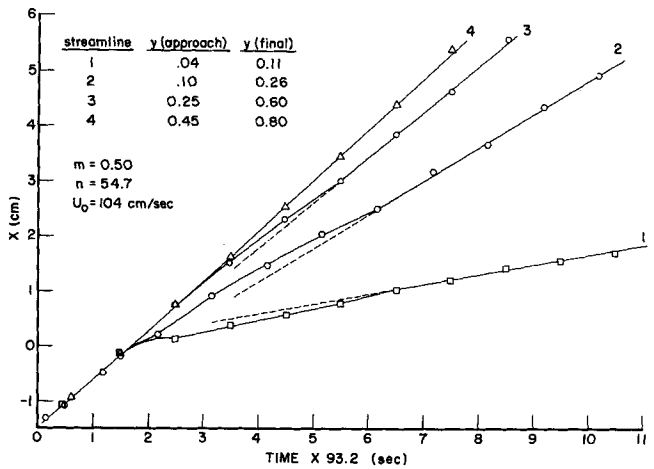

Fig. 5. Particle positions vs. time for viscoelastic fluid (fluid 3).

becomes constant on all four streamlines, indicating that the boundary-layer thickness has reached the outer edge of the jet and that a steady flow has been attained. When a fluid particle on a streamline near the plate surface reaches the leading edge, its velocity decreases steadily to the steady flow value as seen in Figure 6. For the other streamlines a similar behavior is observed, although the transition is not as abrupt, of course. All in all, the type of behavior is as predicted by Newtonian boundary-layer theory.

Figure 5 shows the particle path vs. time curves for 1.3% CMC. Again it is noted that a steady velocity is obtained along all streamlines a few centimeters down the plate. However, it is observed that the distance down the plate required for steady flow to be attained is considerably longer than for the corn syrup solution even though the apparent viscosity of the CMC is less than that of the corn syrup. A more striking difference is noted in the behavior of the velocity near the leading edge. Along the first streamline, which is very close to the plate, the velocity decreases below the steady state velocity, then increases above it, and finally decreases and approaches the steady state velocity. Along the second streamline the velocity decreases relatively slowly (compared to Newtonian behavior) to a value below the steady velocity and then increases and approaches it. The straight line portion of the curve (that is, steady velocity portion) is extrapolated back to help emphasize the effect. As the streamlines get farther from the plate, the effect gets smaller and virtually disappears. Thus, the primary differences between the elastic and the inelastic solutions are found near the leading edge and near the surface of the plate. A sketch of the velocity vs. distance down the plate (x) is given in Figure 6.

Similar results were observed for the 1.0% and 0.7% CMC solutions. However, the effects were smaller for the more dilute solutions.

Since these kinematic anomalies do not appear when the experiment is performed for a Newtonian fluid, and since the anomalous velocity effects increase with increasing elasticity (that is, increasing CMC concentration), it is concluded that they are a result of the elasticity of the fluid. A possible qualitative explanation of this effect is as follows: the approaching fluid suddenly has a large rate of strain imposed on it as it nears the leading edge of the plate, the largest shear rate being near the surface of the plate. Due to the elastic nature of the fluid, the resulting stress is not generated instantaneously, the stress at the leading edge being due principally to the previous low shear rate history of the fluid. Thus, a slower decrease in velocity than for the Newtonian fluid is observed. Then the stress due to these large shear rates begins to mount and the velocity decreases. As the relaxation process sets in, the fluid tends back toward inelastic behavior, since the stress relaxation and generation process begin to take place at nearly the same rate. When the elasticity and shear rate are both high, as for the 1.3% CMC near the plate surface, the imbalance of stress relaxation and generation rates can produce an oscillation in the velocity along a streamline. Unfortunately, because of relatively small diameter of the jet, a steady flow was established, and the process cannot be followed very far down the plate.

Some meaning can also be given to the results by looking at them in terms of the solution of Stokes' problem discussed above. It was observed for the three-constant model that shear stress at the wall was initially less than that of the corresponding Newtonian fluid, but became greater at times of the order of the relaxation time of the fluid. This is precisely the argument used in the intuitive explanation of the kinematical results given above. By measuring the time for a fluid particle to move from the

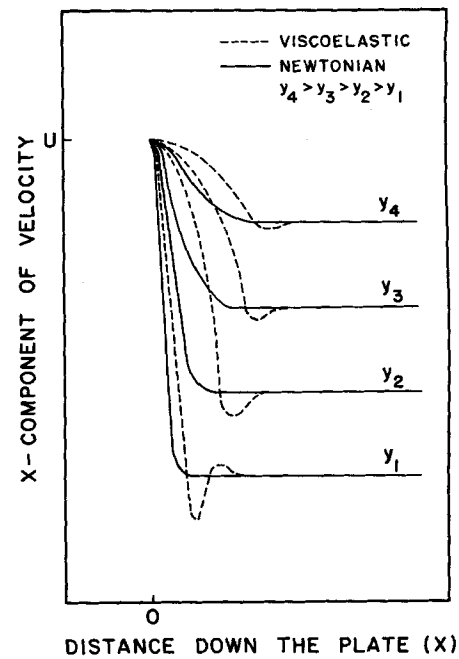

Fig. 6. Schematic diagram of observed kinematic behavior for viscoelastic fluids.

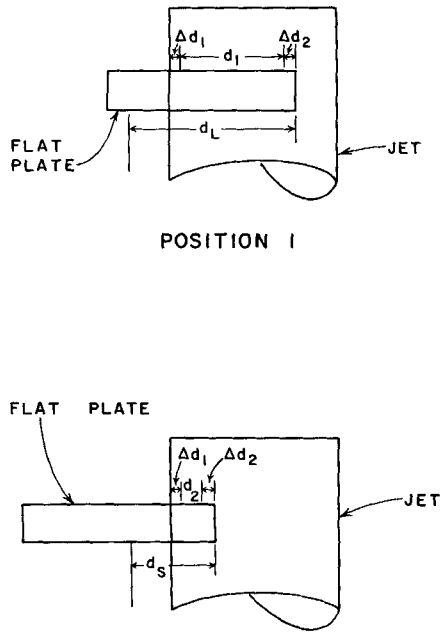

Fig. 7. End and edge effect correction diagram.

leading edge to the point of minimum velocity, one can obtain an estimate of the relaxation time of the fluid. The results showed values of this time to be roughly 0.05 sec. This result corresponds with estimates of relaxation times found in the literature (*13, 30*). Therefore, one can say that the solution of Stokes' problem gives the correct qualitative indication.

Thus, in summary, the large shear rate imposed on the viscoelastic fluid as it flows past the leading edge of the plate causes time-dependent elastic effects which, in turn, produce kinematical disorders. The results of these kinematical measurements indicate that the assumption that the kinematical behavior of moderately viscoelastic fluids is of the same form as that inelastic fluids is incorrect. Thus, order of magnitude analyses such as that made by White and Metzner (*31*) are probably not good for even moderately viscoelastic fluids.

The quantitative effect of these anomalous flow patterns was then investigated by direct measurement of the drag force exerted by the fluid on the plate.

Drag Force Measurements

The drag force on the plate offers a direct test of the applicability of a constitutive equation and the method of solution of the equations of change for flow of viscoelastic fluids past a flat plate. Since the drag force is the variable of chief engineering interest, its accurate prediction is of primary importance. In particular, one wants to know if boundary-layer calculations with the power law model used really describe the physical situation for polymer solutions.

Before comparing the experimental results with theoretical predictions some corrections must be made and some assumptions checked. First of all, true boundary-layer flow does not occur over the entire width of the plate. The force exerted on the plate was measured for the plate extending about ¼ of the way through the jet and also for about ¾ of the way through. Let these distances, referred to a fixed point be d_S and d_L, respectively, and let the corresponding measured forces be F_S and F_L (see Figure 7). Suppose the distance from the edge of the jet to the point where boundary-layer flow occurs over the entire length of the plate is Δd_1 into the jet. Let the average force per unit width on the area be f_{e1}. Also true boundary-layer flow may not exist in the immediate neighborhood of the edge of the plate. Let the distance for which true boundary-layer flow does not exist be Δd_2 and the corresponding force per unit width f_{e2}. It is assumed that true boundary-layer flow occurs over d_1 and d_2. Then

$$f\,d_1 = F_L - f_{e1}\Delta d_1 - f_{e2}\Delta d_2 \tag{12}$$

and

$$f\,d_2 = F_S - f_{e1}\Delta d_2 - f_{e2}\Delta d_2 \tag{13}$$

where f is the force per unit width in true boundary-layer flow. Subtracting, we get

$$f(d_1 - d_2) = F_L - F_S \equiv F \tag{14}$$

but

$$d_1 - d_2 = d_L - d_S = \Delta W \tag{15}$$

then

$$F = f\,\Delta W \tag{16}$$

Thus, the difference between the measured forces is equal to the drag force exerted by boundary-layer flow on a plate of width ΔW.

The problem of calculating the drag force on the plate from theory for various models can be simplified considerably if it can be assumed that the potential velocity U is constant. A photograph of the jet was taken before the plate was inserted into it. The diameter of the jet was measured at positions corresponding to the leading and exit edges of the plate. The corresponding difference in the velocity of the stream was found to be about 4%. Since only large deviations from predictions of inelastic models were of interest, it was decided to use a diameter measure halfway down the plate to calculate the potential velocity. Then this value of the potential velocity was assumed to be constant in the calculations.

Results of Drag Force Measurements

The experimentally measured values of the drag force and those predicted by various inelastic models with the viscometric data of Table 1 used are given in Table 2. In Table 2 F_N is the drag force calculated by using the Blasius solution for the Newtonian model (*27*); F_P is the drag force calculated by using the Acrivos solution for the power law model (*1*); F_E is the calculated drag force by using a Pohlhausen approximation for the modified Ellis model (*11*); and F is the measured drag. The drag force measured for the Newtonian corn syrup is very close to the value predicted by the Newtonian model. This indicates that the measurement and the calculation procedure are good.

On the other hand, it can be seen that the non-Newtonian inelastic models do not predict the drag force for the CMC solutions closely. In fact, the measured value is more than twice the predicted value in all cases. Thus, it can be concluded that the elasticity in the fluid causes the inelastic models to be in serious error near the leading edge of the plate. The error cannot be because of an inadequate description of the non-Newtonian viscosity, because the models used fitted the accurately determined

Table 2. Results of Drag Force Measurements

Fluid	U, cm./sec.	F_E, dynes 10^{-3}	F_P, dynes 10^{-3}	F_N, dynes 10^{-3}	F, dynes 10^{-3}
5	128	—	—	2.33	2.35
8	108	1.24	1.37	—	3.40
7	108	0.90	0.96	—	2.19
6	100	0.52	0.58	—	1.42

viscosity data very well. Therefore, the reason for failure of the power law and Ellis models to describe the actual behavior in both this experiment and the kinematical experiment is certainly that these models neglect the elastic nature of the fluids.

Abnormally large pressure losses in the entrance region of a capillary is a well-established experimental fact (*17, 24, 25*). The large drag force observed in these experiments is a corresponding result. Qualitatively, this increased drag can possibly be explained with reference to the experimental kinematical observations. It was inferred from observations that the stress was generated faster than it could relax near the leading edge of the plate. Since the experimental plate used was quite short, the stress was large over much of the plate. Therefore, a much larger drag force than predicted by purely viscous theory could result. This type of behavior has been also suggested by Metzner and White (*18*) in their discussion of the entrance flow problem.

CONCLUSIONS

Effects of elasticity in the flow of viscoelastic fluids past a flat plate are pronounced near the leading edge of the plate. This is expected, since it is in that region that fluid particles experience the most rapidly changing history of deformation. Experimentally, elasticity is manifested by an oscillation in the velocity along a streamline, and by a drag force which deviates markedly from that predicted by inelastic models. Thus, for short plates, at any rate, inelastic models or approximate calculations based on the assumption that the flow pattern is nearly laminar shear are grossly inaccurate, even in relatively dilute polymer solutions.

The solution of Stokes' problem with linear viscoelastic models used qualitatively explains the experimentally observed phenomena. It is believed that nonlinear models with long memories (integral models) are necessary to accurately describe the flow situation near the leading edge.

At distances farther from the leading edge where the history of deformation is no longer changing so rapidly, the empirical inelastic models are probably sufficient. Use of the second-order viscoelastic model seems to introduce much mathematical complication without much increase in accuracy.

ACKNOWLEDGMENT

The authors are grateful to Dr. John Huppler of the University of Wisconsin for performing viscometric experiments on the fluids studied. They wish to thank Professor R. B. Bird for making the instruments available. R. A. Hermes thanks Hercules Powder Company and the National Science Foundation for providing fellowships for his graduate study. Financial support of the research was provided by the National Science Foundation under Grant GP-799.

NOTATION

a defined by Equation (10)
d_1, d_2, Δd_1, Δd_2 see Figure 7
f, f_{e1}, f_{e2} = forces per unit length
F = corrected drag force
F_E = drag force calculated from modified Ellis model
F_L = drag force measured in position 1
F_N = drag force calculated from Newtonian model
F_P = drag force calculated from power law model
F_S = drag force measured in position 2
G_N, G_M = shear moduli
m, n = power law parameters
m_e, n_e = Ellis model parameters
p, p^{ij}, etc. = shear stress tensor
s = Laplace transform variable
U = free-stream velocity
t = time
u = x component of velocity
x^i = current coordinates
X^i = material coordinates
$-$ = Laplace transforms of quantities

Greek Letters

Γ_1 = rate of strain tensor
Γ_2 = convected derivative of Γ_1
ΔW = corrected plate width
δ = Dirac delta function
η = viscosity
η_0 = zero shear viscosity
λ = relaxation time
ρ = density
ψ = relaxation function
ω_2, ω_3 = material functions

LITERATURE CITED

1. Acrivos, Andreas, M. J. Shah, and E. E. Peterson, *A.I.Ch.E. J.*, **6**, 312 (1960).
2. ————, *Chem. Eng. Sci.*, **20**, 101 (1965).
3. Bizzell, G. D., and J. C. Slattery, *ibid.*, **17**, 777 (1962).
4. Clutter, D. W., O. M. Smith, and J. G. Brazier, *Aerospace Eng.*, **20** (1961).
5. Coleman, B. D., R. J. Duffin, and V. J. Mizel, *Arch. Rat. Mech. Anal.*, **19**, 100 (1965).
6. Coleman, B. D., and Walter Noll, *ibid.*, **3**, 289 (1959).
7. ————, *Ann. N. Y. Acad. Sci.*, **89**, 672 (1961).
8. Etter, Irwin, and W. R. Schowalter, *Trans. Soc. Rheol.*, **9**, Pt. 2, 351 (1965).
9. Fredrickson, A. G., "Principles and Applications of Rheology," Prentice-Hall, Englewood Cliffs, N. J. (1964).
10. Green, A. E., and R. S. Rivlin, *Arch. Rat. Mech. Anal.*, **1**, 1 (1957).
11. Hermes, R. A., Ph.D. thesis, Univ. Minnesota, Minneapolis (1965).
12. Huppler, J. D., Ph.D. thesis, Univ. Wisconsin, Madison (1965).
13. Kalb, J. W., Ph.D. thesis, Univ. Minnesota, Minneapolis (1967).
14. Kapoor, N. N., J. W. Kalb, E. A. Brumm, and A. G. Fredrickson, *Ind. Eng. Chem. Fundamentals*, **4**, 186 (1965).
15. Kline, S. J., et al, *Dept. Mech. Eng. Rept. No. MD-10* (1964).
16. McEachern, D. W., Ph.D. thesis, Univ. Wisconsin, Madison (1963).
17. Metzner, A. B., W. T. Houghton, R. A. Sailor, and J. L. White, *Trans. Soc. Rheol.*, **5**, 133 (1961).
18. Metzner, A. B., and J. L. White, *A.I.Ch.E. J.*, **11**, 989 (1965).
19. Rajeswari, G. K., and S. L. Rathna, *Z. Angew. Math. Phys.*, **13**, 43 (1962).
20. Reiner, Markus, "Deformation, Strain, and Flow," Interscience, New York (1960).
21. Rivlin, R. S., *J. Rat. Mech. Anal.*, **5**, 179 (1956).
22. ———, and J. L. Ericksen, *ibid.*, **4**, 323 (1955).
23. Sadowski, T. J., Ph.D. thesis, Univ. Wisconsin, Madison (1963).
24. Sakiadis, B. C., *A.I.Ch.E. J.*, **8**, 317 (1962).
25. *Ibid.*, **9**, 706 (1963).
26. Savins, J. G., and K. Walters, *Trans. Soc. Rheol.*, **9**, 407 (1965).
27. Schlichting, Hermann, "Boundary Layer Theory," McGraw-Hill, New York (1960).
28. Schowalter, W. R., *A.I.Ch.E. J.*, **6**, 24 (1960).
29. Sutterby, J. L., *Trans. Soc. Rheol.*, **9**, Pt. 2, 227 (1965).
30. Vela, Saul, J. W. Kalb, and A. G. Fredrickson, *A.I.Ch.E. J.*, **11**, 288 (1965).
31. White, J. L., and A. B. Metzner, *ibid.*, **11**, 324 (1965).

Manuscript received June 1, 1966; revision received August 15, 1966; paper accepted August 15, 1966.